Diffusion Parameters in the Striatum of Rats With 6-Hydroxydopamine–Induced Lesions and With Fetal Mesencephalic Grafts

T. Reum,[1] F. Olshausen,[1] T. Mazel,[2,3] I. Voříšek,[2,3] R. Morgenstern,[1] and
E. Syková[2,3]★

[1]Institute of Pharmacology and Toxicology, Medical Faculty (Charité), Humboldt-University, Berlin, Germany
[2]Institute of Experimental Medicine, Academy of Sciences of the Czech Republic, Vídenská, Prague,
Czech Republic
[3]Department of Neuroscience, 2nd Medical Faculty, and Center for Cell Therapy and Tissue Repair,
Charles University, Prague, Czech Republic

Functional recovery after transplantation of dopaminergic cells into the lesioned striatum is dependent on widespread diffusion of the transmitter released by the graft. In the present study, we investigated the diffusion parameters of the extracellular space in the striatum of control, 6-hydroxydopamine-lesioned, intrastriatally grafted, and sham-grafted rats in vivo. We used two types of grafts—single macrografts or multiple micrografts. The real-time iontophoretic tetramethylammonium method enabled us to extract three extracellular space diffusion parameters: volume fraction, α, tortuosity, λ, and nonspecific uptake of tetramethylammonium, k'. Compared with controls ($\alpha = 0.19$, $\lambda = 1.59$), in lesioned animals both α and λ were lower ($\alpha = 0.14$, $\lambda = 1.50$). α and λ were increased inside macro- and micrografts, where $\alpha = 0.24$ and $\lambda = 1.80$, and in sham-grafted areas, where $\alpha = 0.24$ and $\lambda = 1.72$. In regions outside the grafts ($\alpha = 0.15$, $\lambda = 1.51$) or in sham grafts ($\alpha = 0.14$, $\lambda = 1.49$), the values of α and λ were similar to the values observed in lesioned striatum. Nonspecific uptake (k') did not differ among the groups. Our results show that, compared with control, α and λ were decreased in dopamine-depleted areas and increased in areas with grafts. Multiple but smaller graft deposits, in contrast to their enlarged capability for dopaminergic reinnervation, impair the conditions for diffusion and extrasynaptic transmission in a larger area of the striatum than do single macrografts, presumably because of more extensive tissue damage, cell loss, and astrogliosis.
© 2002 Wiley-Liss, Inc.

Key words: extrasynaptic transmission; Parkinson's disease; tortuosity; transplantation; volume fraction

Volume transmission of dopamine (DA) plays an important role in the nigrostriatal system (Fuxe and Agnati, 1991; Yung et al., 1995; Zoli and Agnati, 1996; Gonon, 1997; Zoli et al., 1998; Nicholson and Syková, 1998). Although dopaminergic terminals form small symmetric synapses en passant on spines of striatal medium spiny neurons (Freund et al., 1985; Groves et al., 1994), only a fraction of DA receptors in the striatum is directly associated with synaptic structures (Sesack et al., 1994; Yung et al., 1995). The impact of DA on D1 receptors (Gonon, 1997) as well as neuronal high-affinity uptake of DA occurs outside the synaptic cleft (Garris et al., 1994; Nirenberg et al., 1996). Volume transmission is of great importance in states of striatal DA depletion (Bjelke et al., 1994; Zoli et al., 1998; Strömberg et al., 2000), and sufficient DA diffusion up to distances of several millimeters has been observed in experimental models of Parkinson's disease (PD; Schneider et al., 1994).

The unilateral intracerebral injection of 6-hydroxydopamine (6-OHDA) in rats producing a selective degeneration of catecholaminergic neurons (Ungerstedt, 1968) is a widely used animal model of PD. DA agonists induce a characteristic rotational behavior (Ungerstedt and Arbuthnott, 1970) because of the asymmetric dopaminergic lesion and up-regulated striatal DA receptors (Ungerstedt, 1971). This model was used to demonstrate functional recovery by intrastriatal transplantation of fetal dopaminergic cells for the first time (Björklund and Steveni, 1979; Perlow et al., 1979). Fetal mesencephalic grafts have been shown to ameliorate parkinsonian symptoms in patients (for review see Lindvall, 1998), and the use of stem cells

for neurotransplantation is a significant future option for treatment of PD (Gage, 2000).

Although graft-induced recovery in the parkinsonian brain is generally related to the sprouting of tyrosine hydroxylase (TH)-positive fibers and synapse formation (for review see Björklund, 1992; Herman and Abrous, 1994), there is experimental evidence for graft-induced effects outside the area of histologically verified reinnervation by grafted cells. Normalization of DA–neuropeptide Y interactions (Vuillet et al., 1994) and of up-regulated D2 receptors (Strömberg et al., 2000) is explained by widespread diffusion of graft-derived DA through the extracellular space (ECS). Cell grafting into the brain is accompanied by tissue injury and followed by a variety of pathological tissue reactions that can markedly influence the diffusion properties. An astrogliotic reaction and scar as assessed by glial fibrillary acidic protein (GFAP) immunohistochemistry are found in stab wounds of the brain (Barker et al., 1996; Roitbak and Syková, 1999), at the graft–host interface of mesencephalic grafts in the striatum (Nikkhah et al., 1994b; Barker et al., 1996), and in cortical grafts (Syková et al., 1999a). Astrogliosis in the grafted brain causes ECS changes (Syková et al., 1999a) that could impair the diffusion of transmitters, drugs, and nutrients. However, it has been shown that the extent of graft-derived striatal astrogliosis depends on the grafting technique. Weaker histological signs of astrogliosis were found in rat brains when the so-called microtransplantation approach was used (Nikkhah et al., 1994b; Brandis et al., 1998). The intrastriatal injection of more and smaller mesencephalic cell deposits via a very thin glass capillary, rather than the use of a conventional metal cannula to inject two large cell deposits, is the most important difference between this modified technique and the standard macrotransplantation technique. It is hypothesized that the minimized tissue trauma and the reduced tissue inflammation resulting from microtransplantation in comparison with macrotransplantation are responsible for the reduced astrogliosis and the improved survival of grafted dopaminergic cells (Nikkhah et al., 1994a,b), but there are no data on the ECS characteristics and functional diffusion conditions in the grafted striatum.

The aim of this study was to investigate the striatal diffusion in normal, parkinsonian, and intrastriatally grafted or sham-grafted rats. We used 6-OHDA-lesioned rats and performed both intrastriatal microtransplantation and macrotransplantation to assess further whether differences in the diffusion properties were evident following either grafting technique. The ECS diffusion characteristics can be properly described by the ECS volume fraction and tortuosity (Syková, 1997; Nicholson and Syková, 1998). Volume fraction is defined as the ratio of ECS volume to total tissue volume (α = ECS volume/total tissue volume). Tortuosity (λ) is calculated as the ratio between the free diffusion coefficient (D) and the apparent diffusion coefficient in the tissue (ADC): $\lambda^2 = D/ADC$. Tortuosity summarizes the hindrances imposed by cellular structures, molecules of the extracellular matrix, and the

connectivity of different spaces. In the present study, we used the tetramethylammonium (TMA) method (Nicholson and Phillips, 1981). This method is based on real-time concentration measurements of an iontophoretically applied extracellular marker, TMA, using TMA^+-sensitive microelectrodes and may elucidate the functional diffusion conditions in normal, DA denervated, grafted, and sham-grafted rat striatum in vivo.

MATERIALS AND METHODS

In all animal experiments, every effort was made to minimize animal suffering and the number of animals used. Experiments were carried out in accordance with the European Communities Council Directive of 24 November 1986 (86/609/ EEC). German governmental permission is registered under No. G 0106/99.

Time Line of the Experimental Protocol

Male Wistar rats (Harlan-Winkelmann, Borchen, Germany) were lesioned with 6-OHDA at the age of 7 weeks to produce a unilateral parkinsonian disease pathology. A group of control animals was left intact. Five weeks after the 6-OHDA injection, i.e., at the age of 12 weeks, all lesioned animals were tested for their rotational behavior, and animals showing stable rotations after systemic injection of amphetamine were considered as properly lesioned and accepted for further studies. A group of lesioned animals was left without any other treatment; the rest were grafted with fetal dopaminergic cells (E14) or sham-grafted at the age of 13 weeks. Six and twelve weeks after grafting, i.e., at the ages of 19 and 25 weeks, the animals were tested again for rotational behavior. ECS diffusion parameters were measured in vivo at the ages of 7–9 months. Immediately after these measurements, the animals were perfused and their brains processed for histology. The experiments were performed with three different sets of rats. Each set containing 20–25 rats underwent all steps of this experimental protocol separately. The rats of each set were distributed into all five different treatment groups after the lesion and each set also included control rats. Only those rats being subject to all experiments within the time line and showing no irregularities during the different steps of this study were included for final statistical analysis.

6-OHDA Lesions

Male Wistar rats (7 weeks old; Harlan-Winkelmann, Borchen, Germany) were pretreated with pargyline (Sigma, Deisenhofen, Germany; 50 mg/kg i.p.) and desipramine (RBI, Natick, MA; 25 mg/kg i.p.), anesthetized with pentobarbital (Sigma; 35 mg/kg i.p.), and mounted in a stereotaxic frame. Stereotaxic coordinates (A, anterior, -4.4 mm; L, lateral, 1.1 mm; V, ventral, 7.6 mm) were determined vs. bregma and the cerebral surface according to the atlas of Paxinos and Watson (1986). The tooth bar was set 2.4 mm below interaural zero. A small hole was drilled through the skull and 6-OHDA hydrochloride (Sigma; 8 μg in 1 μl 0.9% saline containing 0.1% ascorbic acid) was injected via a stainless steel cannula (outer diameter 0.23 mm) into the medial forebrain bundle of the left hemisphere over 1 min. The cannula was left in place for another 5 min before retracting it slowly and closing the wound.

Rotational Behavior

The functional effect of 6-OHDA lesioning and of the ensuing grafting was tested by evaluating the rotational behavior of the rats after D-amphetamine (Sigma; 2 mg/kg i.p.) injection. Rotations were recorded by automatic "rotameters" (TSE, Bad Homburg, Germany) over a period of 60 min starting 15 min after amphetamine injection, and their count was defined as follows: Each circular movement exceeding 30° was registered. Ipsilateral (toward the lesioned side) and contralateral movements (toward the nonlesioned side) were counted, then divided by 12 to calculate the full (360°) number of rotations. Finally, the net number of rotations was determined by calculating the difference between ipsilateral and contralateral rotations.

Animals showing a mean of five ipsilateral rotations per minute or more were considered as properly lesioned (Hefti et al., 1980) and were used for further experiments. The rats were distributed randomly into five counterbalanced groups. Two groups received ventral mesencephalic cell transplantations into the lesioned striatum, and two parallel groups received sham grafts and were treated and tested analogously to the grafted animals. The fifth group received no further treatment after the lesion. A control group of age-matched rats remained untreated; i.e., no lesioning or grafting was performed. Each group finally consisted of 5–10 animals.

Grafting Procedure

According to the protocol of Dunnett and Björklund (1997), the ventral mesencephalon was dissected from rat embryos of the same strain at day E 14 and collected in cold 0.9% NaCl solution supplemented with 0.6% glucose (SG). The tissue underwent an enzymatic digestion with 1% trypsin (Sigma) and 0.1% DNAse (Sigma) in SG for 20 min at 37°C. After repeated washes in SG, a cell suspension was made by repeated aspiration through small, flame-polished pipette tips with consecutively decreasing diameters. After a brief centrifugation (66g, 4°C, 4 min), the supernatant was carefully suctioned off. The cells were resuspended in SG with 0.01%DNAse in a final volume of 7.5 μl per mesencephalon, corresponding to 65,000–100,000 cells/μl. The final suspension was kept cold and light protected to be used within 4 hr for transplantation. After transplantation was finished, the proportion of viable cells was still $\geq$80% as evaluated by acidine orange and ethidium bromide in the hemocytometer using a fluorescence microscope.

Host rats were anesthetized with pentobarbital (50 mg/kg i.p.; Sigma) and mounted into a stereotaxic frame. For macrotransplantation, two deposits of the suspension containing 2 μl each were injected into the striatum at the following coordinates according to the atlas of Paxinos and Watson (1986): A, 1.0 mm; L, 3.0 mm vs. bregma to depths of 5.0 mm and 4.1 mm below the cortical surface, tooth bar set at −5 mm below the interaural level. The suspension was injected with a 10 μl Hamilton microsyringe via a stainless steel cannula (outer diameter 0.47 mm) over 2 min into each deposit, and the cannula was left in place for an additional 5 min before slowly raising or retracting it. Sham-grafted controls received an injection of the vehicle (SG with 0.01% DNAse) only.

For microtransplantation, the cannula was connected with a pulled glass capillary (outer diameter 0.06−0.08 mm at the tip) as described by Nikkhah et al. (1994b), and eight deposits, each containing 0.5 μl of the same cell suspension as used for macrotransplantation, were implanted at the following coordinates: A, 0 mm and 1 mm vs. bregma, L, 2.3 and 3.3 mm vs. bregma to a depth of 5.0 and 4.1 mm below the cortical surface, tooth bar set at −5 mm below the interaural level. After slow injection of the suspension (30 sec per each deposit), the capillary was left in place for additional 3 min before slowly retracting it. Sham-grafted controls received an injection of vehicle (SG with 0.01% DNAse) at the same coordinates.

Measurement of ECS Diffusion Parameters

ECS diffusion parameters were evaluated in vivo at the age of 7–9 months in the striatum of control (n = 10), 6-OHDA-lesioned (n = 5), sham-grafted (n = 6), and grafted (n = 10) rats. The real-time iontophoretic method was used to determine the ECS volume fraction α, tortuosity λ, and nonspecific uptake k' (Nicholson and Syková, 1998). Briefly, TMA$^+$, a substance to which cell membranes are relatively impermeable, was administered via an iontophoretic micropipette into the nervous tissue (Fig. 1). Iontophoretic pipettes were made from theta glass tubing (Clark Electromedical Instruments England) and filled with 100 mM TMA$^+$. The concentration of TMA$^+$ was then measured by means of a double-barreled TMA$^+$-sensitive microelectrode (TMA$^+$-ISM) at a distance of 100−200 μm from the tip of the iontophoretic electrode.

TMA$^+$-ISMs were prepared by a procedure described previously (for details see Syková et al., 1999a). The ion exchanger was a Corning 477317, and the ion-sensitive barrel was backfilled with 100 mM TMA$^+$ chloride (Sigma, Prague, Czech Republic). The reference barrel contained 150 mM NaCl. The shank of the iontophoretic electrode was bent so that it could be aligned parallel to the TMA$^+$-ISM. The TMA$^+$-ISM and the iontophoretic micropipette were then glued together using dental cement.

Rats were anesthetized with chloral hydrate (400 mg/kg) and mounted into a stereotaxic frame with the tooth bar set at the same horizontal plane as the ear bars. The different head positions of the rats used for transplantation and the measurement of diffusion parameters ensured that the ion-sensitive electrode passed the former transplantation tract at an angle of approximately 10°. The skull and dura over the striatum were removed, and the electrodes were lowered into the striatum. Skull impressions resulting from the former drill holes for transplantation were used as orientation points for appropriate electrode placement. TMA$^+$ was applied using a 24 sec or 60 sec iontophoretic current step of 80 or 180 nA. To maintain a stable background of the probe ion, a bias current of +20 nA was delivered continuously. Potentials recorded at the reference barrel of the ion-selective microelectrode were subtracted from the ion-selective barrel potentials by means of buffer and subtraction amplifiers. The resulting diffusion curves were analyzed using the program VOLTORO (Nicholson, unpublished). TMA$^+$ diffusion curves were initially recorded in a cup filled with 0.3% agar in 150 mM NaCl, 3 mM KCl, and 1 mM TMA chloride. This allowed us to determine the electrode array transport number and TMA$^+$ free diffusion coefficient. TMA$^+$ diffusion curves were then recorded at various depths of the
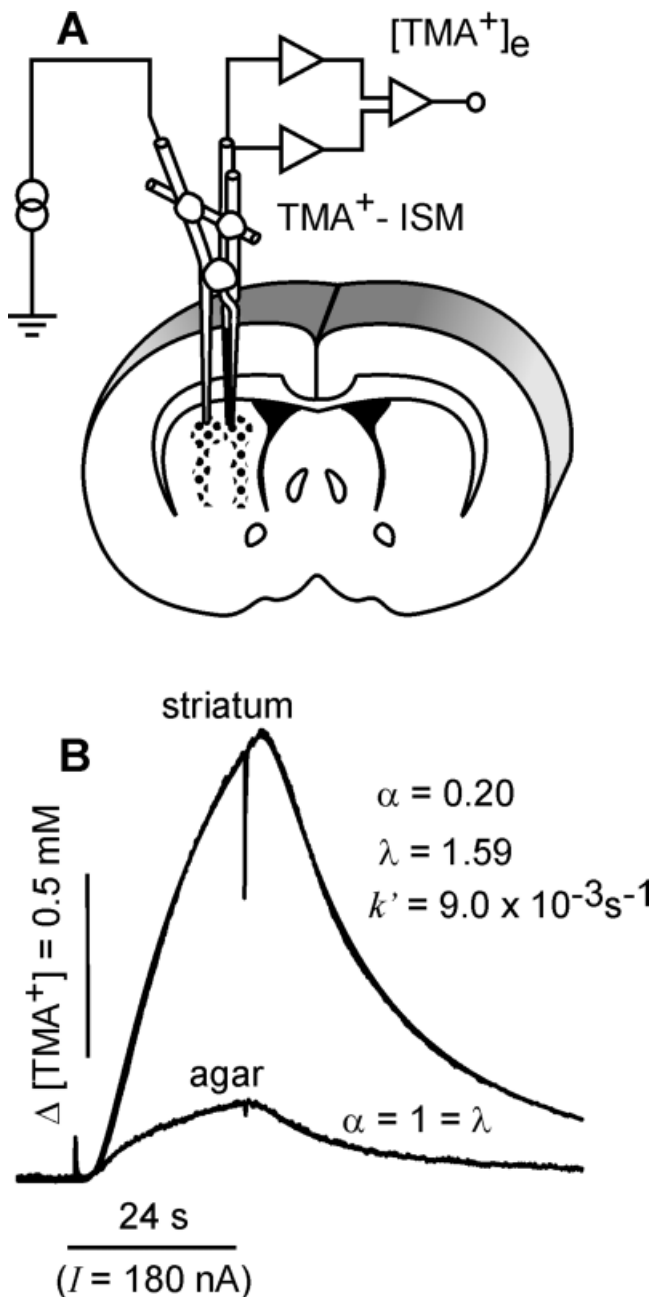
Fig. 1. Measurement of ECS diffusion parameters. **A:** Experimental arrangement for the real-time iontophoretic TMA$^+$ method. A TMA$^+$-selective, double-barreled, ion-selective microelectrode (TMA$^+$-ISM) was glued to a bent iontophoretic micropipette filled with 100 mM TMA Cl. The typical intertip distance was 100–200 μm. **B:** Typical diffusion curves obtained in 0.3% agar and in the rat striatum. An 80 nA iontophoretic current was used to expel TMA$^+$ from the tip of the iontophoretic pipette. Voltage changes at the TMA$^+$-selective microelectrode corresponding to concentration changes were recorded and fit according to the radial diffusion equation to yield the ECS volume fraction (α) and tortuosity (λ). Agar calibration (α = 1 = λ) enabled us to determine the TMA$^+$ free diffusion coefficient (D) and the electrode transport number.

striatum along one or more tracks and analyzed to yield α, λ, and k'. The diffusion measurements were designed so that, in the striatum of grafted rats, both the 6-OHDA-lesioned environment outside the graft and the graft itself were crossed by the microelectrode. Assignment of individual data to a location inside or outside the graft/sham graft was made by final histological track reconstruction performed in the appropriate brain slices.

Immunohistochemistry of TH and GFAP

Immediately after the measurement of ECS diffusion parameters, the rats under deep general anesthesia (500 mg/kg chloral hydrate i.p.) were intracardially perfused with 80 ml phosphate-buffered saline (PBS; 0.042 M Na$_2$HPO$_4$, 0.008 M NaH$_2$PO$_4$ · H$_2$O, 0.15 M NaCl, pH 7.7), followed by 200 ml of ice-cold 4% paraformaldehyde in PBS. The brains were removed, postfixed in the same fixative, and dehydrated in 20% sucrose in PBS. Serial coronal sections (30 μm) were cut on a freezing microtome and processed for free-floating TH and GFAP immunohistochemistry. For TH staining, slices were rinsed three times with 0.05 M Tris buffer (TB; pH 7.6), quenched with 3% H$_2$O$_2$/10% methanol in TB for 15 min, and rinsed three times with TB. After a preincubation with 5% normal goat serum (NGS)/0.3% Triton/TB, the sections were incubated with the primary antibody (1:500, anti-TH; Calbiochem, Nottingham, United Kingdom) in 2% NGS/TB overnight at 4°C. After three rinses with TB, the sections were incubated with a biotinylated goat anti-rabbit IgG (1:200; Sigma) in TB for 2 hr, rinsed again three times with TB, and stained with 0.05% diaminobenzidine/0.03% H$_2$O$_2$/TB for 5–10 min. The sections were mounted onto gelatin-coated slides, dehydrated in ascending alcohol concentrations, and coverslipped.

For GFAP staining, an alternate set of sections was rinsed in PBS, quenched with 0.6% H$_2$O$_2$ in PBS for 15 min, and preincubated with 0.2% Triton/PBS for 1 hr. Incubation was performed with the primary antibody (1:50, anti-GFAP; Boehringer-Mannheim, Mannheim, Germany) in combination with 0.1% albumin and 0.02% Triton in PBS at 4°C overnight. After three rinses with PBS, the floating sections were incubated with biotinylated anti-mouse IgG (1:200)/0.02% Triton/PBS for 2 hr at room temperature, rinsed again three times with PBS, and finally incubated with peroxidase-labeled avidin-biotin (1:100)/0.02% Triton/PBS for 1 hr at room temperature (Vectastain Elite; Vector Laboratories, Burlingame, CA). After three rinses with PBS, the immune complexes were visualized using 0.05% 3,3′-diaminobenzidine tetrachloride (Sigma) in 0.05 M Tris buffer (pH 7.6) and 0.02% H$_2$O$_2$ for 2–4 min. The sections were mounted onto gelatin-coated slides, dehydrated, and coverslipped.

The number of TH-immunoreactive cells in the grafted striatum was determined by counting all TH-positive neuronal cell bodies under a microscope in brightfield illumination. Every third or fourth section through the grafted striatum was stained and counted. The number of counted neurons was corrected according to the formula of Abercrombie (1946). Graft dimensions, TH-positive fiber sprouting, and the degree and localization of astrogliosis were qualitatively assessed. Reconstruction of the electrode track was performed in GFAP-stained slices to

determine whether and at what depth the graft was crossed by the ion-sensitive microelectrode. The substantia nigra pars compacta (SNC) was checked for loss of TH-positive cells.

Statistical Analysis

Within the sham-grafted and grafted groups, the numbers of amphetamine-induced rotations before and after transplantation and sham transplantation were compared with each other by repeated-measures ANOVA and post hoc Tukey test. $P < 0.05$ was considered to be statistically significant.

The ECS parameters α, λ, and k' were averaged for each individual animal first. Based on GFAP staining, histological track analysis allowed the assignment of individual data to the corresponding location inside or outside the grafts. For grafted and sham-grafted animals, these data were averaged separately. The obtained mean values representative for one animal and for the respective striatal subregion if necessary were assigned to the treatment groups to be statistically compared with each other using one-way ANOVA and post hoc multiple-comparisons procedures (Dunnett's test) vs. controls. $P < 0.05$ was considered to be statistically significant.

Some animals had to be excluded from statistical analysis. Either these animals died before the experiment was finished or a certain post mortem track analysis was not possible.

RESULTS

Rotational Behavior

Five weeks after 6-OHDA lesion, most of the rats showed a strong amphetamine-induced rotational behavior. We observed 5.9 ± 0.5 ipsilateral rotations per minute (mean $\pm$ SEM, four groups, n = 46). There was no difference in the number of rotations between the treatment groups. Grafting of mesencephalic cells into the lesioned striatum markedly reduced the number of amphetamine-induced ipsilateral rotations (Fig. 2) and eventually produced net contralateral rotations. In macro-grafted rats (n = 13), 0.4 ipsilateral rotations and 1.5 contralateral rotations were recorded per minute when tested 6 and 12 weeks after grafting, respectively. For micrografted rats (n = 10), we observed a mean number of 2.4 contralateral turns per minute 6 weeks after grafting and 4.5 contralateral turns per minute 12 weeks after grafting. At these time points, no significant differences in rotational behavior were found between macrografted and micrografted rats. After sham grafting (n = 11 and 12 for sham-micrografted and sham-macrografted rats, respectively), the number of rotations was significantly increased in both groups at both tested time points (Fig. 2).

Immunohistochemical Analysis of Lesions, Grafts, and Sham Grafts

We found in the SNC an almost complete degeneration of TH-positive neurons in the lesioned hemisphere (Fig. 3A). Some single TH-positive cells were found in a few animals, but the absolute number was very low in those rats. In the striatum of macrografted animals, the grafted TH-positive cells were organized in one elongated graft, about 0.2–0.4 mm wide and 2.0–2.5 mm
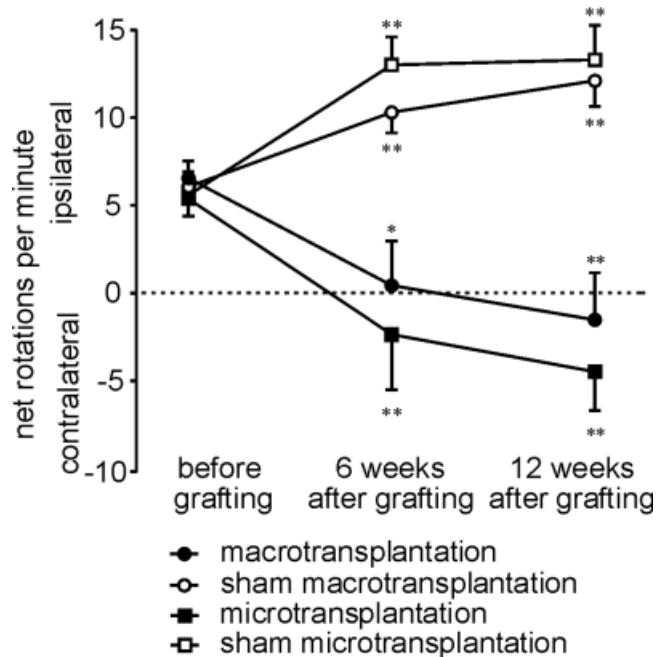
Fig. 2. Amphetamine-induced rotational behavior in 6-OHDA-lesioned and intrastriatally grafted or sham-grafted rats. Data are expressed as numbers (mean $\pm$ SEM) of ipsilateral (toward the lesioned side) or contralateral (toward the nonlesioned side) rotations per minute. $\star P < 0.05$, $\star\star P < 0.01$, repeated-measures ANOVA and post hoc Tukey test.

long. The cells occurred loosely in the periphery of the graft and tended to form clusters (Fig. 3B). From these cells, TH-positive fibers sprouted toward both the inside and the outside of the graft, with an estimated average range of about 250 μm but in individual cases even up to 1 mm. The mean number of TH-positive cells in macro-grafted rats was 556 (range 140–991 cells). GFAP staining revealed an increased gliotic reaction in the grafted area, usually extending over an area of 150–300 μm, with a typical dense strip of GFAP activity surrounding the grafts. The strip, of about 25–50 μm thickness, was found at the

Fig. 3. Coronal sections of lesioned and grafted brains showing TH-positive cells in the ventral midbrain (**A**) and in the grafted striatum (**B,D**) as well as striatal GFAP activity after grafting (**C,E**). A: Degeneration of DAergic cells in the substantia nigra pars compacta (SNC) and ventral tegmental area (VTA) following a 6-OHDA lesion (left) compared with TH-positive DA cells in the SNC (beneath asterisks) and in the VTA (arrowheads) of the nonlesioned hemisphere. B,D: In the grafted striatum, TH-positive cells (arrowheads) were found in single deposits after macrotransplantation (B) or in several deposits after microtransplantation (D). Sprouting of TH-positive fibers (arrows) from the graft–host interface toward both the inside and the outside of the graft. C,E: Serial sections stained for GFAP from macrografted (C) and micrografted (E) rats show an increased reaction inside the grafts and a typical GFAP-positive strip at the graft host border (arrows in C). CC, corpus callosum; V, ventricle.
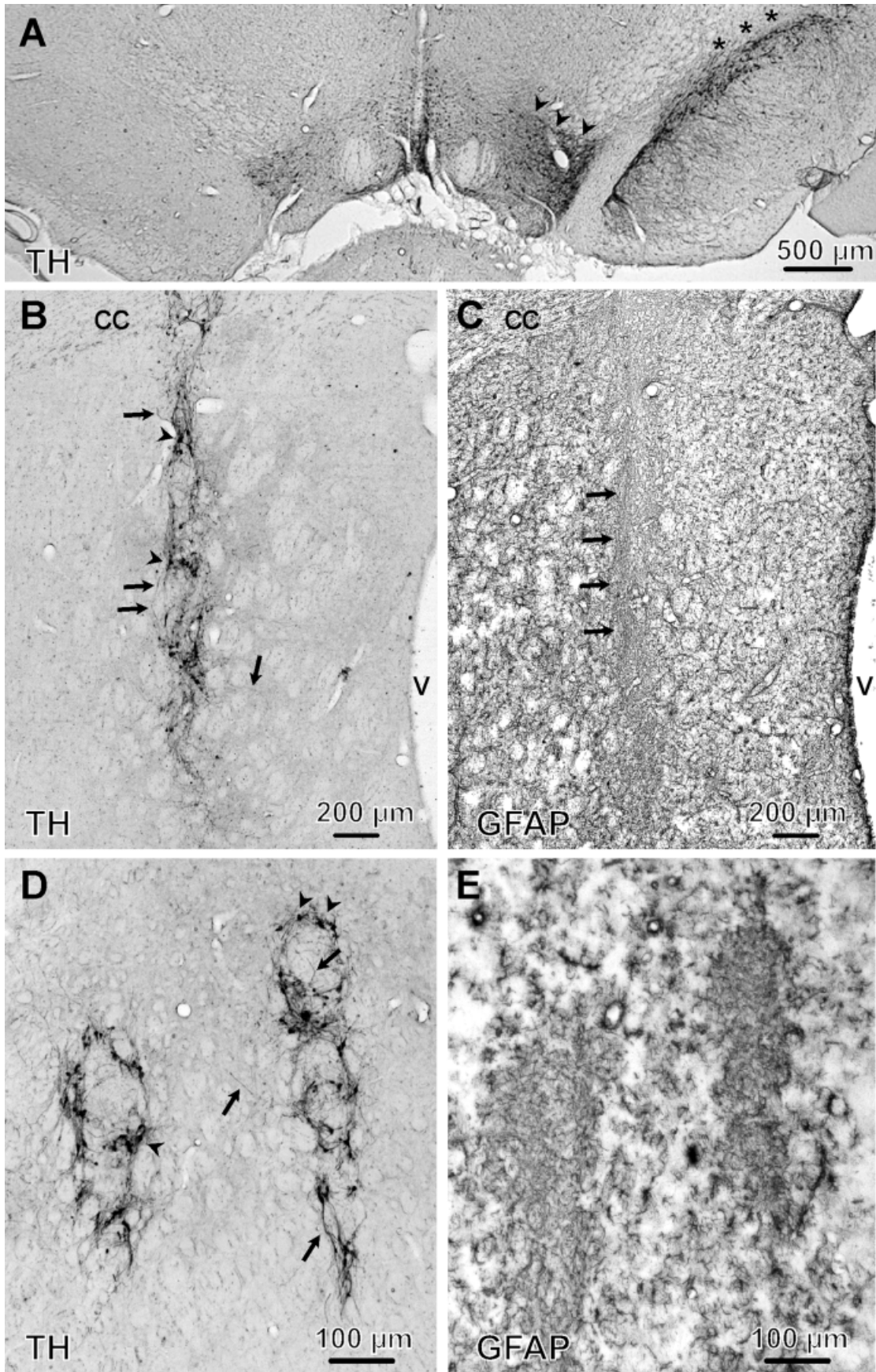
Figure 3.

edge of grafts in the area of many TH-positive cells (Fig. 3C).

TH-positive cells in micrografted animals were found in separate tracks, but a confluence of single cell deposits along one track was observed in these animals too. A mean number of 653 (range 208–1,148) TH-positive cells was calculated from cell counts in microtransplants. The cells were loosely distributed in the graft, and their tendency to localize in the periphery was less pronounced in comparison with macrotransplants. A dense sprouting of TH-positive fibers, extending from the graft–host interface, was observed both toward the inside and toward the outside of the graft (Fig. 3D).

A gliotic tissue reaction occurred in the proximity of both transplants (Fig. 3C,E) and sham grafts (see Figs. 5B, 6B). In general, GFAP was closely related to the needle track and to the placement of fetal cells or vehicle solution, respectively (see Figs. 5A,B, 6A,B).

Diffusion Parameters in the Lesioned and Grafted Striatum

ECS volume fraction α, tortuosity λ and nonspecific uptake k' were measured in vivo in control, 6-OHDA-lesioned, sham-grafted, and grafted rats. Measurements were performed at various depths of the striatum in 200 μm steps from 3 to 5 mm below the brain surface.

Figures 4–6 represent individual experiments in control, 6-OHDA-lesioned, macro- and micrografted, and sham macro- and micrografted animals, showing values of α and λ at various depths of the striatum, representative TMA$^+$ diffusion curves, and GFAP-stained coronal sections. The position of the electrode tracks is marked with arrowheads.

Figure 4 shows experiments in a control and a 6-OHDA-lesioned rat. Diffusion curves recorded in the striatum of the lesioned animal were higher than the diffusion curves recorded in the control rat (Fig. 4E,F); i.e., the ECS volume fraction was lower in the lesioned animal. In the control animal, α was about 0.20 and λ about 1.65, whereas, in the lesioned one, both parameters were decreased to about 0.14 and 1.45, respectively (Fig. 4C,D).

In macrografts and sham macrografts, the area of transplantation is characterized by marked astrogliosis, revealed by increased GFAP staining in Figure 5A,B. Figure 5 shows that, in both experiments, the electrode penetrated the astrogliotic graft area at a depth of 3.7 mm. In the macrograft, particularly high values of α and λ were observed near the border of the transplant. α and λ were also elevated inside the sham macrograft (Fig. 5C,D). Outside the grafts and sham grafts, the ECS diffusion parameters were similar to those observed in lesioned-only animals.

In micrografts and sham micrografts, eight deposits of fetal mesencephalic cell suspension were made within four tracks. Two tracks characterized by increased GFAP staining are visible in Figure 6A,B. The ECS diffusion parameters showed an increase in α and λ similar to that in the macrografted and sham-macrografted animals (Fig. 6C–F).

Table I summarizes the results of the diffusion measurements. The mean ECS volume fraction, tortuosity, and nonspecific uptake in control rats were $\alpha = 0.19$, $\lambda = 1.59$, and $k' = 0.01$ sec^{-1}, respectively. These values did not significantly differ from those found previously either in vivo, where $\alpha = 0.22$ and $\lambda = 1.54$ (Jansson et al., 1999), or in vitro, where $\alpha = 0.21$ and $\lambda = 1.54$ (Rice and Nicholson, 1991). Both α and λ were significantly lower in lesioned animals as well as in areas outside the grafts or sham grafts; α ranged from 0.14 to 0.15 and λ from 1.49 to 1.51. In grafts and sham grafts, both parameters were higher than in areas outside them and were in fact even higher than in control striatum; the mean value of α was 0.24, and λ ranged from 1.72 to 1.80. No significant differences in nonspecific uptake were found in any of the groups compared with controls. We did not find any significant difference in ECS parameters when rats with microtransplants and macrotransplants or their corresponding sham-grafted counterparts were compared with each other (Figs. 5E, 6E). Therefore, we pooled the animals into one grafted group and one sham-grafted group.

DISCUSSION

Our study compares the extracellular diffusion parameters in the striatum of control, 6-OHDA-lesioned, grafted, and sham-grafted rats. Amphetamine-induced rotational behavior was used as a rough functional test to verify the effectiveness of lesioning and grafting before final histological post mortem analysis was performed. Only properly lesioned animals, showing five or more ipsilateral rotations per minute after D-amphetamine injection, were selected for further experiments (Hefti et al., 1980). In accordance with many studies reviewed by Björklund (1992) and by Herman and Abrous (1994), successful grafting led to a reduction in the rotation number and a reversed direction of amphetamine-induced turning in 6-OHDA-lesioned rats. In our study, the rotational behavior did not reveal significantly better recovery in micrografted vs. macrografted rats. The consequences of the different grafting techniques for the striatal ECS diffusion parameters are discussed below.

We found, in the striatum of lesioned rats as well as in the lesioned areas outside the grafts or sham grafts, a significant decrease in λ and α in comparison with untreated controls. This change implies improved diffusion-based volume transmission of DA in areas of DA depletion; a lower λ means easier diffusion, and a lower α results in a relative increase in the extracellular concentration of substances. Furthermore, the prolongation of extracellular DA clearance by the loss of DA uptake sites after 6-OHDA lesions (van Horne et al., 1992; Garris et al., 1997) would allow for more extensive diffusion of the transmitter. Indeed, widespread diffusion of DA has been demonstrated in the DA-depleted striatum (Schneider et al., 1994). It is difficult to relate the changes in ECS diffusion parameters to any previously observed morpho-

Control

A

6-OHDA lesion

B

C

D

E

$\alpha = 0.20$

$\lambda = 1.60$

control

24 s

$(I = 180\ nA)$

F

$\alpha = 0.14$

$\lambda = 1.45$

lesioned

24 s

$(I = 180\ nA)$
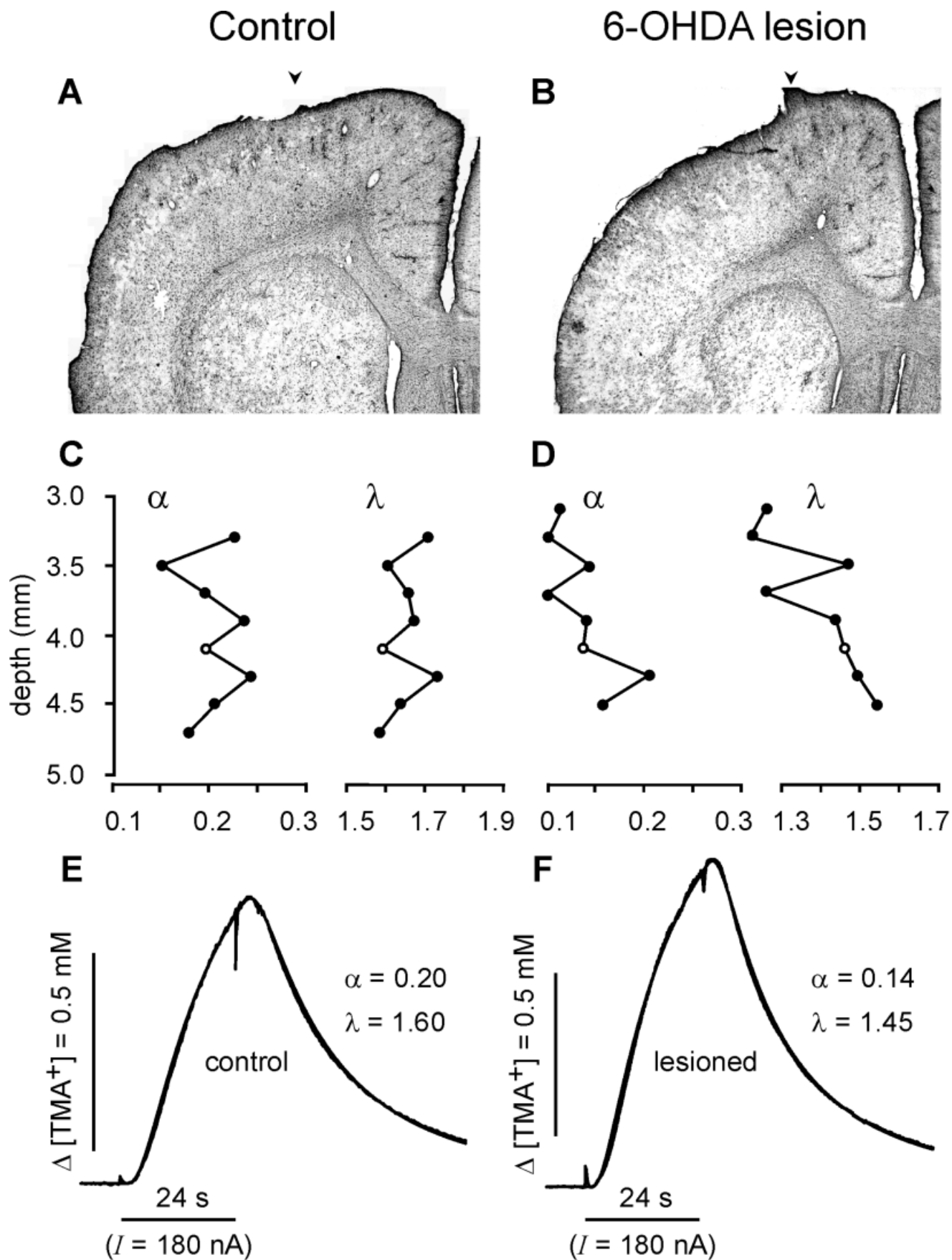
Fig. 4. Typical experiments in a control (**A,C,E**) and a 6-OHDA-lesioned (**B,D,F**) animal. A,B: Coronal sections stained for GFAP. Microelectrode penetrations are marked with arrowheads. C,D: ECS diffusion parameters recorded in the striatum plotted against the depth of measurement (0 level corresponds to the brain surface). E,F: TMA$^+$ diffusion curves recorded at the depths indicated by the open circles in C,D. Note that both α and λ were lower in 6-OHDA-lesioned rats than in control animals. The electrode transport numbers and intertip distances were, in C,E, n = 0.307 and r = 163 μm and, in D,F, n = 0.293 and r = 160 μm.
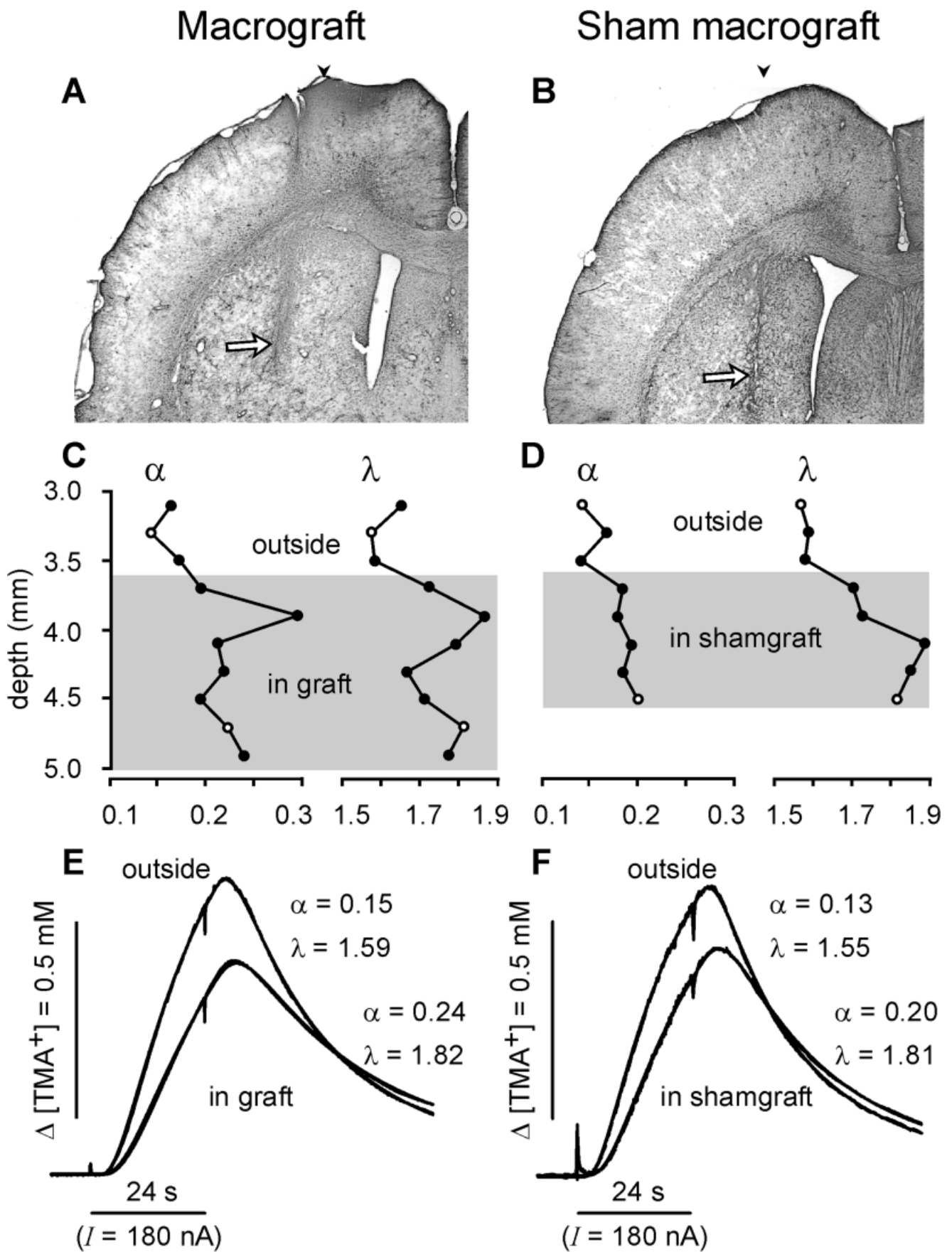
Figure 5.

logical changes in the lesioned striatum. However, arte-factual changes of ECS parameters by lesion surgery can be excluded, insofar as striatal degeneration of DA terminals was produced by a small 6-OHDA injection close to the dopaminergic neurons in the midbrain and not by affecting the striatum directly. Gates et al. (1996) found no changes in the intensity of staining for GFAP, chondroitin sulfate proteoglycans, or tenascin in 6-OHDA-lesioned animals compared with controls. However, functional changes have been observed. The decrease in ECS volume fraction might be related to the observed up-regulation of spontaneous activity in noninnervated areas (Strömberg et al., 2000). Increased neuronal activity is known to produce a decrease in ECS volume fraction (Svoboda and Syková, 1991). The degeneration of more than 75% of neurons in this structure leads to a progressive loss of DA terminals (Finkelstein et al., 2000) and a loss of spines on striatal target neurons (Ingham et al., 1998). These changes may in part explain the observed decrease in ECS tortuosity. A similar decrease in both α and λ was observed during aging (Syková et al., 1998, 2002). This decrease was attributed mainly to astrocytic changes—thicker processes and enlarged cell bodies—and to a decrease in the content of extracellular matrix molecules.

Different changes were observed inside the fetal mesencephalic grafts and sham grafts, where both α and λ increased and even exceeded values in control animals. The strong similarity of the increases in λ and α in grafted and sham-grafted rats indicates that tissue injury and astrogliosis are the main causes of the altered state of the ECS. Indeed, a comparable increase of both α and λ was found after stab wounding of the cerebral cortex (Roitbak and Syková, 1999). Although the increase in α is related to injury and cell death, astrogliosis and accompanying changes in extracellular matrix are probably the most important reason for the increase of λ inside grafts and sham grafts as demonstrated previously in cortical and tectal tissue transplantation (Syková et al., 1999a). Hypertrophied astrocytes were found throughout the entire graft but were most prominent at the graft–host border of mesencephalic suspension grafts (Fig. 3), in accordance with findings of Nikkhah et al. (1994b) and Barker et al.

(1996). Reactive astrocytes also produce a variety of extracellular matrix molecules, including sulfated proteoglycans, tenascin, and vitronectin (Barker et al., 1996; Roitbak and Syková, 1999; Syková et al., 1999b, 2000). These molecules may hinder diffusion and also push cells apart (Syková et al., 1999a) and thus may substantially contribute to the increase in both α and λ. In agreement with our findings, electron microscopic investigations revealed that grafted DA cells are often isolated from the surrounding tissue by astrocytes or by spaces (Bolam et al., 1987). The diffusion parameters in regions outside of the grafts remained as in lesioned striatum, and these regions showed no signs of astrogliosis.

What might be the functional consequences of such a situation in the grafted striatum? An increase in α inside the grafts leads to a quicker dilution of any released substance, whereas the increase in λ means decreased diffusion of transmitters and drugs (Syková et al., 1999a). The release of DA is very high inside the grafts (Earl et al., 1996; Cragg et al., 2000), but the activity of DA transporters in grafts is accordingly high (Wang et al., 1994; Cragg et al., 2000). The consequence of a higher α and λ and the increased activity of DA transporters within the grafts would be a reduced DA "source strength" provided by the dopaminergic graft. Furthermore, the diffusion of drugs into the graft may be impaired (Zoli et al., 1999). However, better diffusion conditions for DA exist in the surrounding tissue. In addition to favorable changes in ECS geometry, there is an extension of the extracellular life of DA because of reduced uptake activity in the lesioned areas (van Horne et al., 1992; Garris et al., 1997; Cragg et al., 2000).

When micrografted and macrografted rats or their sham-grafted counterparts were compared with each other, no significant differences were found in ECS diffusion parameters, in rotational behavior, or in the number of surviving TH-positive cells. With regard to cell survival and histological characterization, our results are in contrast to those from Nikkhah et al. (1994a), who found a significantly enhanced number of surviving dopaminergic cells after microtransplantation. Furthermore, in macrotransplants, the so-called core area, a morphologic region showing either sparse or no TH-positive cells (Nikkhah et al., 1994a), was less pronounced, and the graft morphology appeared to be rather similar for macrotransplants and microtransplants in our study. Some methodological deviations may explain these differences. We used a slightly thicker capillary for microtransplantation and generally grafted lower cell numbers. The microtransplanted rats also received a lower number of transplantation tracks and deposits in our study (8 instead of 18), which was necessary to maintain the possibility of histological track reconstruction. However, we believe based on our results that neither a different size and shape of the grafts nor a greater number of grafted cells will significantly change the diffusion properties inside the graft, because, in grafted rats, the number of TH-positive cells did not correlate with the ECS parameters (data not shown), and all groups of grafted

Fig. 5. Typical experiments in a macrografted (**A,C,E**) and a sham-macrografted animal (**B,D,F**). A,B: Coronal sections stained for GFAP. Grafted and sham-grafted areas are characterized by intensive GFAP staining (arrows). Microelectrode penetration is marked with arrowheads. C,D: ECS diffusion parameters recorded in the striatum plotted against the depth of measurement (0 level corresponds to the brain surface). Areas inside grafts and sham grafts are shaded in gray. Both α and λ were increased in astrogliotic areas inside the grafts and sham grafts. In contrast, both parameters were lower in the DA-depleted surrounding tissue. E,F: TMA$^+$ diffusion curves recorded at the depths indicated by the open circles in C,D. Note the higher α and λ values inside the graft and sham graft compared with the areas of 6-OHDA-lesioned striatum (outside). The electrode transport numbers and intertip distances were, in C,E, $n = 0.303$ and $r = 183$ μm and, in D,F, $n = 0.297$ and $r = 175$ μm.

Micrograft

A

C

α λ

depth (mm)

3.0
3.5 — outside
4.0
4.5 — in graft
5.0

0.1 0.2 0.3 1.5 1.7 1.9

E

outside

Δ [TMA$^+$] = 0.5 mM

α = 0.14
λ = 1.56

in graft

α = 0.26
λ = 1.84

60 s

(I = 180 nA)

Sham micrograft

B

D

α λ

outside

in shamgraft

0.1 0.2 0.3 1.5 1.7 1.9

F

outside

Δ [TMA$^+$] = 0.5 mM

α = 0.15
λ = 1.37

α = 0.29
λ = 1.65

in shamgraft

60 s

(I = 180 nA)
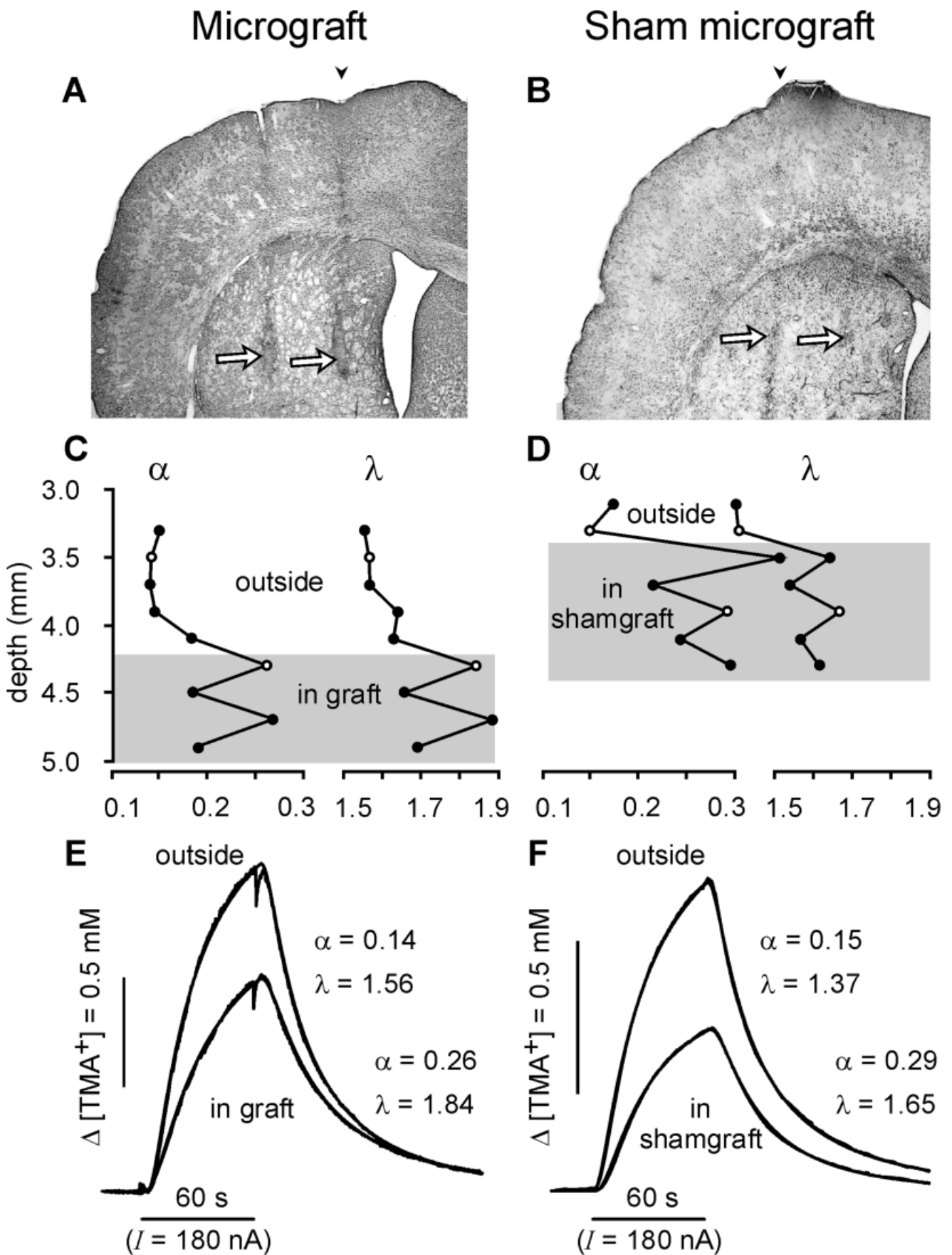
Figure 6.

TABLE I. Mean Values of Extracellular Space Diffusion Parameters in the Striatum of Control, 6-Hydroxydopamine-Lesioned, Fetal Mesencephalic Grafted, and Sham-Grafted Rats[†]

	n/N	α	λ	k' ($\times 10^{-3}$)
Controls	10/116	0.19 ± 0.03	1.59 ± 0.05	10 ± 4
6-OHDA-lesioned rats	5/48	0.14 ± 0.02★	1.50 ± 0.06★	9 ± 3
Grafted rats				
Inside the graft	8/68	0.24 ± 0.05★	1.80 ± 0.08★	6 ± 4
Outside the graft	9/91	0.15 ± 0.02★	1.51 ± 0.06★	9 ± 4
Sham-grafted rats				
Inside the sham graft	5/41	0.24 ± 0.04★	1.72 ± 0.06★	10 ± 4
Outside the sham graft	6/54	0.14 ± 0.02★	1.49 ± 0.04★	9 ± 5

[†]Data are expressed as mean ± S.D. n, Number of animals; N, number of measurements. Results obtained in macro- and micrografted and sham-macro-and -micrografted animals have been pooled.
★$P < 0.05$ vs. control.

and sham-grafted rats showed the same consistent changes in ECS parameters.

Our data suggest that high DA reinnervation inside the graft, with increased hindrances for volume transmission, stands in opposition to DA-depleted areas outside the graft, with fewer diffusion barriers. This situation ought to support and improve DA diffusion in the lesioned areas. This hypothesis seems to be of primary relevance for macrotransplants. However, the main purpose of using the microtransplantation technique is to enlarge the area of reinnervation by the grafted cells. The use of thin instruments for microtransplantation is known to reduce astrogliosis in the single transplantation tract (Nikkhah et al., 1994b; Brandis et al., 1998). In our study, this was observed as well. However, we did not quantify the overall extent of striatal astrogliosis after grafting, but it appeared to be larger in micrografted animals, because the transplantation was made in 4 tracks. This technique may provide more DA cells throughout the lesioned striatum, but at the same time it impairs the conditions for volume transmission in this area. This could be one reason for observations that, in microtransplanted rats, the remarkable extension of reinnervated areas and of dopaminergic transmission in the striatum (Nikkhah et al., 1994a) is not accompanied by marked improvements in the recovery of complex sensorimotor behavior (Nikkhah et al., 1998).

The concept of an extreme extension of grafted cell deposits into the DA-depleted striatum has to be critically scrutinized, because our data confirm impaired diffusion conditions in every striatal region suffering mechanical injury. A balanced amount and distribution of grafted tissue in the lesioned striatum and strategies to reduce astrogliosis and other mechanisms that impair ECS geometry for diffusion should be found and developed. This not only would improve volume transmission and drug diffusion but also would allow better sprouting of fibers from grafted DA cells.

It is important to note that the ECS diffusion parameters we report here relate simply and solely to the diffusion of TMA. Direct in vivo investigations of extrasynaptic DA diffusion from grafted cells into the lesioned striatum should be the subject of future studies to determine the role of volume transmission in functional recovery from dopamine depletion.

ACKNOWLEDGMENTS

Fig. 6. Typical experiments in a micrografted (**A,C,E**) and a sham-micrografted animal (**B,D,F**). A,B: Coronal sections stained for GFAP. Grafted and sham-grafted areas are characterized by intensive GFAP staining (arrows). Microelectrode penetration is marked with arrowheads. C,D: ECS diffusion parameters recorded in the striatum plotted against the depth of measurement (0 level corresponds to the brain surface). Areas inside grafts and sham grafts are shaded in gray. Both α and λ were increased in astrogliotic areas inside the grafts and sham grafts. In contrast, both parameters were lower in the DA-depleted surrounding tissue. E,F: TMA$^+$ diffusion curves recorded at the depths indicated by the open circles in C,D. Note the higher α and λ values inside the graft and sham graft compared with the areas of 6-OHDA-lesioned striatum (outside). The electrode transport numbers and intertip distances were, in C,E, n = 0.331 and r = 180 μm and, in D,F, n = 0.343 and r = 200 μm.

REFERENCES

Abercrombie M. 1946. Estimation of nuclear population from microtome sections. Anat Rec 94:239–247.

Barker RA, Dunnett SB, Faissner A, Fawcett JW. 1996. The time course of loss of dopaminergic neurons and the gliotic reaction surrounding grafts of embryonic mesencephalon to the striatum. Exp Neurol 141:79–93.

Bjelke B, Strömberg I, O'Connor WT, Andbjer B, Agnati L, Fuxe K. 1994. Evidence for volume transmission in the dopamine denervated neostriatum of the rat after a unilateral nigral 6-OHDA microinjection. Studies with systemic D-amphetamine treatment. Brain Res 662:11–24.

Björklund A. 1992. Dopaminergic transplants in experimental parkinsonism: cellular mechanisms of graft-induced functional recovery. Curr Opin Neurobiol 2:683–689.

Björklund A, Steveni U. 1979. Reconstruction of the nigrostriatal pathway by intracerebral nigral transplants. Brain Res 177:555–560.

Bolam JP, Freund TF, Björklund A, Dunnett SB, Smith AD. 1987. Synaptic input and local output of dopaminergic grafts that functionally reinnervate the host neostriatum. Exp Brain Res 68:131–146.

Brandis A, Kuder H, Knappe U, Jödicke A, Schönmayr R, Samii M, Walter GF, Nikkhah, G. 1998. Time dependent expression of donor- and host-specific major histocompatibility complex class I and II antigens in allogeneic dopamine-rich macro- and micrografts: comparison of two different grafting protocols. Acta Neuropathol 95:85–97.

Cragg SJ, Clarke DJ, Greenfield SA. 2000. Real-time dynamics of dopamine released from neuronal transplants in experimental Parkinson's disease. Exp Neurol 164:145–153.

Dunnett SB, Björklund A. 1997. Basic neural transplantation techniques. I. Dissociated cell suspension grafts of embryonic bentral mesencephalon in the adult rat brain. Brain Res Prot 1:91–99.

Earl CD, Reum T, Xie JX, Kupsch A, Oertel WH, Morgenstern R. 1996. Influences of foetal nigral cell suspension grafts on the dopamine release in the nongrafted side in the 6-hydroxydopamine rat model of parkinsons disease: in vivo voltammetric data. Exp Brain Res 109:179–184.

Finkelstein DI, Stanic D, Parish CL, Tomas D, Dickson K, Horne MK. 2000. Axonal sprouting following lesions of the rat substantia nigra. Neuroscience 97:99–112.

Freund TF, Bolam JP, Björklund A, Steveni U, Dunnett SB, Powell JF, Smith AD. 1985. Efferent synaptic connections of grafted dopaminergic neurons reinnervating the host neostriatum: a tyrosine hydroxylase immunocytochemical study. J Neurosci 5:603–616.

Fuxe K, Agnati L. 1991. Two principal modes of electrochemical communication in the brain: volume versus wiring transmission. In: Fuxe K, Agnati L, editors. Volume transmission in the brain. Novel mechanisms for neural transmission. Advances in neuroscience, vol 1. New York: Raven Press. p 1–9.

Gage FH. 2000. Mammalian neural stem cells. Science 287:1433–1438.

Garris PA, Ciolkowski EL, Pastore P, Wightman RM. 1994. Efflux of dopamine from the synaptic cleft in the nucleus accumbens of the rat brain. J Neurosci 14:6084–6093.

Garris PA, Walker QD, Wightman RM. 1997. Dopamine release and uptake rates both decrease in the partially denervated striatum in proportion to the loss of dopamine terminals. Brain Res 753:225–234.

Gates MA, Laywell ED, Fillmore H, Steindler DA. 1996. Astrocytes and extracellular matrix following intracerebral transplantation of embryonic ventral mesencephalon or lateral ganglionic eminence. Neuroscience 74:579–597.

Gonon F. 1997. Prolonged and extrasynaptic excitatory action of dopamine mediated by D1 receptors in the rat striatum in vivo. J Neurosci 17:5972–5978.

Groves PM, Linder JC, Young SJ. 1994. 5-Hydroxydopamine-labeled dopaminergic axons: three dimensional reconstructions of axons, synapses and postsynaptic targets in rat neostriatum. Neuroscience 58:593–604.

Hefti F, Melamed E, Wurtman RJ. 1980. Partial lesions of the dopaminergic nigrostriatal system in rat brain: biochemical characterization, Brain Res 195:123–137.

Herman JP, Abrous ND. 1994. Dopaminergic neural grafts after fifteen years: results and perspectives. Progr Neurobiol 44:1–35.

Ingham CA, Hood SH, Taggart P, Arbuthnott GW. 1998. Plasticity of synapses in the rat neostriatum after unilateral lesion of the nigrostriatal dopaminergic pathway. J Neurosci 18:4732–4743.

Jansson A, Mazel T, Andbjer B, Rosén L, Guidolin D, Zoli M, Syková E, Agnati L, Fuxe K. 1999. Effects of nitric oxide inhibition on the spread of biotinylated dextran and on extracellular space parameters in the neostriatum of the male rat. Neuroscience 91:69–80.

Lindvall O. 1998. Update on fetal transplantation: the Swedish experience. Mov Disord 13:83–87.

Nicholson C, Phillips JM. 1981. Ion diffusion modified by tortuosity and volume fraction in the extracellular microenvironment of the rat cerebellum. J Physiol 321:225–257.

Nicholson C, Syková E. 1998. Extracellular space structure revealed by diffusion analysis. Trends Neurosci 21:207–215.

Nikkhah G, Cunningham MG, Jödicke A, Knappe U, Björklund A. 1994a. Improved graft survival and striatal reinnervation by microtransplantation of fetal nigral cell suspensions in the rat Parkinson model. Brain Res 633:133–143.

Nikkhah G, Olsson M, Eberhard J, Bentlage C, Cunningham MG, Björklund A. 1994b. A microtransplantation approach for cell suspension grafting in the rat Parkinson model: a detailed account of the methodology. Neuroscience 63:57–72.

Nikkhah G, Rosenthal C, Falkenstein G, Samii M. 1998. Dopaminergic graft-induced long term recovery of complex sensorimotor behaviors in a rat model of Parkinson's disease. Zentralbl Neurochir 59:97–103.

Nirenberg MJ, Vaughan RA, Uhl GR, Kuhar MJ, Pickel VM. 1996. The dopamine transporter is localized to dendritic and axonal plasma membranes of nigrostriatal dopaminergic neurons. J Neurosci 16:436–447.

Paxinos G, Watson C. 1986. The rat brain in stereotaxic coordinates. New York: Academic Press.

Perlow MI, Freed WJ, Hoffer BJ, Seiger A, Olson L, Wyatt RJ. 1979. Brain grafts reduce motor abnormalities produced by destruction of nigrostriatal dopamine system. Science 204:643–647.

Rice ME, Nicholson C. 1991. Diffusion characteristics and extracellular volume fraction during normoxia and hypoxia in slices of rat neostriatum. J Neurophysiol. 65:264–272.

Roitbak T, Syková E. 1999. Diffusion barriers evoked in the rat cortex by reactive astrogliosis. Glia 28:40–48.

Schneider JS, Rothblat DS, DiStefano L. 1994. Volume transmission of dopamine over large distances may contribute to recovery from experimental parkinsonism. Brain Res 643:86–91.

Sesack SR, Aoki C, Pickel VM. 1994. Ultrastructural localization of D2-receptor-like immunoreactivity in midbrain dopamine neurons and their striatal targets. J Neurosci 14:88–106.

Strömberg I, Kehr J, Andbjer B, Fuxe K. 2000. Fetal ventral mesencephalic grafts functionally reduce the dopamine D2 receptor supersensitivity in partially dopamine reinnervated host striatum. Exp Neurol 164:154–165.

Svoboda J, Syková E. 1991. Extracellular space volume changes in the rat spinal cord produced by nerve stimulation and peripheral injury. Brain Res 560:216–224.

Syková E. 1997. The extracellular space in the CNS: its regulation, volume and geometry in normal and pathological neuronal function. Neuroscientist 3:28–41.

Syková E, Mazel T, Šimonová Z. 1998. Diffusion constraints and neuron–glia interaction during aging. Exp Gerontol 33:837–851.

Syková E, Roitbak T, Mazel T, Šimonová Z, Harvey AR. 1999a. Astrocytes, oligodendroglia, extracellular space volume and geometry in rat fetal brain grafts. Neuroscience 91:783–798.

Syková E, Vargová L, Prokopová Š, Šimonová Z. 1999b. Glial swelling and astrogliosis produce diffusion barriers in the rat spinal cord. Glia 25:56–70.

Syková E, Mazel T, Vargová L, Voříšek I, Prokopová Š. 2000. Extracellular space diffusion and pathological states. Progr Brain Res 125:155–178.

Syková E, Mazel T, Hasenöhrl RU, Harvey AR, Šimonová Z, Mulders WHAM, Huston JP. 2002. Memory deficit in aged rats correlates with impared diffusion parameters in hippocampus. Hippocampus 12:469–479.

Ungerstedt U. 1968. 6-Hydroxy-dopamine induced degeneration of central monoamine neurons. Eur J Pharmacol 5:107–110.

Ungerstedt U. 1971. Striatal dopamine release after amphetamine or nerve degeneration revealed by rotational behaviour. Acta Physiol Scand 367(Suppl):49–68.

Ungerstedt U, Arbuthnott GW. 1970. Quantitative recording of rotational behavior in rats after 6-hydroxy-dopamine lesions of the nigrostriatal dopamine system. Brain Res 24:485–493.

van Horne C, Hoffer BJ, Strömberg I, Gerhardt GA. 1992. Clearance and diffusion of locally applied dopamine in normal and 6-hydroxydopamine-lesioned rat striatum. J Pharmacol Exp Ther 263:1285–1292.

Vuillet J, Moukhles H, Nieoullon A, Daszuta A. 1994. Ultrastructural analysis of graft-to-host connections, with special reference to dopamine–neuropeptide Y interactions in the rat striatum, after transplantation of fetal mesencephalon cells. Exp Brain Res 98:84–96.

Wang Y, Wang SD, Lin SZ, Liu JC. 1994. Restoration of dopamine overflow and clearance from the 6-hydroxydopamine lesioned rat striatum reinnervated by fetal mesencephalic grafts. J Pharmacol Exp Ther 270:814–821.

Yung KKL, Bolam JP, Smith AD, Hersch SM, Ciliax J, Levey AI. 1995. Immunocytochemical localization of D1 and D2 dopamine receptors in the basal ganglia of the rat: light and electron microscopy. Neuroscience 65:709–730.

Zoli M, Agnati LF. 1996. Wiring and volume transmission in the central nervous system: the concept of closed and open synapses. Progr Neurobiol 49:363–380.

Zoli M, Torri C, Ferrari R, Jansson A, Zini I, Fuxe K, Agnati LF. 1998. The emergence of the volume transmission concept. Brain Res Rev 26:136–147.

Zoli M, Jansson A, Syková E, Agnati LF, Fuxe K. 1999. Volume transmission in the CNS and its relevance for neuropsychopharmacology. Trends Pharmacol Sci 20:142–150.